

# Systematic analysis of interannual and seasonal variations of model-simulated tropospheric NO<sub>2</sub> in Asia and comparison with GOME-satellite data

I. Uno<sup>1</sup>, Y. He<sup>2</sup>, T. Ohara<sup>3</sup>, K. Yamaji<sup>4</sup>, J.-I. Kurokawa<sup>3</sup>, M. Katayama<sup>3</sup>, Z. Wang<sup>5</sup>, K. Noguchi<sup>6</sup>, S. Hayashida<sup>6</sup>, A. Richter<sup>7</sup>, and J. P. Burrows<sup>7</sup>

<sup>1</sup>Research Institute for Applied Mechanics, Kyushu University, Kasuga Park 6-1, Kasuga, Fukuoka, Japan

<sup>2</sup>Earth System Science and Technology, Kyushu University, Kasuga Park 6-1, Kasuga, Fukuoka, Japan

<sup>3</sup>National Institute for Environmental Studies, Tsukuba, Ibaraki, Japan

<sup>4</sup>Frontier Research Center for Global Change, Japan Agency for Marine-Earth Science and Technology, Yokohama, Japan

<sup>5</sup>NZC/LAPC, Institute of Atmospheric Physics, Chinese Academy of Sciences, Beijing, China

<sup>6</sup>Information Science, Faculty of Science, Nara Women's University, Nara, Japan

<sup>7</sup>Institute of Environmental Physics, University of Bremen, Bremen, Germany

Received: 14 September 2006 – Published in Atmos. Chem. Phys. Discuss.: 10 November 2006

Revised: 15 February 2007 – Accepted: 20 March 2007 – Published: 27 March 2007

**Abstract.** Systematic analyses of interannual and seasonal variations of tropospheric NO<sub>2</sub> vertical column densities (VCDs) based on GOME satellite data and the regional scale chemical transport model (CTM), Community Multi-scale Air Quality (CMAQ), are presented for the atmosphere over eastern Asia between 1996 and June 2003. A newly developed year-by-year emission inventory (REAS) was used in CMAQ. The horizontal distribution of annual averaged GOME NO<sub>2</sub> VCDs generally agrees well with the CMAQ results. However, CMAQ/REAS results underestimate the GOME retrievals with factors of 2–4 over polluted industrial regions such as Central East China (CEC), a major part of Korea, Hong Kong, and central and western Japan. The most probable reasons for the underestimation typically over the CEC are accuracy of the basic energy statistic data, emission factors, and socio-economic data used for construction of emission inventory. For the Japan region, GOME and CMAQ NO<sub>2</sub> data show reasonable agreement with respect to interannual variation and show no clear increasing trend. For CEC, GOME and CMAQ NO<sub>2</sub> data indicate a very rapid increasing trend from 2000. Analyses of the seasonal cycle of NO<sub>2</sub> VCDs show that GOME data have larger dips than CMAQ NO<sub>2</sub> during February–April and September–November. Sensitivity experiments with fixed emission intensity reveal that the detection of emission trends from satellite in fall or winter has a larger error caused by the variability of meteorology. Examination during summer time and annual averaged NO<sub>2</sub> VCDs are robust with respect to variability of meteorology

and are therefore more suitable for analyses of emission trends. Analysis of recent trends of annual emissions in China shows that the increasing trends of 1996–1998 and 2000–2002 for GOME and CMAQ/REAS show good agreement, but the rate of increase by GOME is approximately 10–11% yr<sup>-1</sup> after 2000; it is slightly steeper than CMAQ/REAS (8–9% yr<sup>-1</sup>). The greatest difference was apparent between the years 1998 and 2000: CMAQ/REAS only shows a few percentage points of increase, whereas GOME gives a greater than 8% yr<sup>-1</sup> increase. The exact reason remains unclear, but the most likely explanation is that the emission trend based on the Chinese emission related statistics underestimates the rapid growth of emissions.

## 1 Introduction

Examination of long-term tropospheric NO<sub>2</sub> variation plays an important role in analysis of recent increases of NO<sub>x</sub> emissions over Asia. Because the NO<sub>2</sub> lifetime is short and the effects of horizontal transport in the continental boundary layer are small, it is reasonable to discuss the relationship between NO<sub>x</sub> emission inventory and satellite NO<sub>2</sub> vertical column densities (VCDs). Richter et al. (2005) warned of the impact of rapid emission increases over China based on their Global Ozone Monitoring Experiment (GOME) satellite-derived NO<sub>2</sub> columns. They show that the trend of increase is approximately of the order of 7% yr<sup>-1</sup> from 1996 to 2002, implying an almost 40% increase within seven years. At the same time, GOME NO<sub>2</sub> columns show little variation in other areas and agree well with ground-based

Correspondence to: I. Uno  
(uno@riam.kyushu-u.ac.jp)

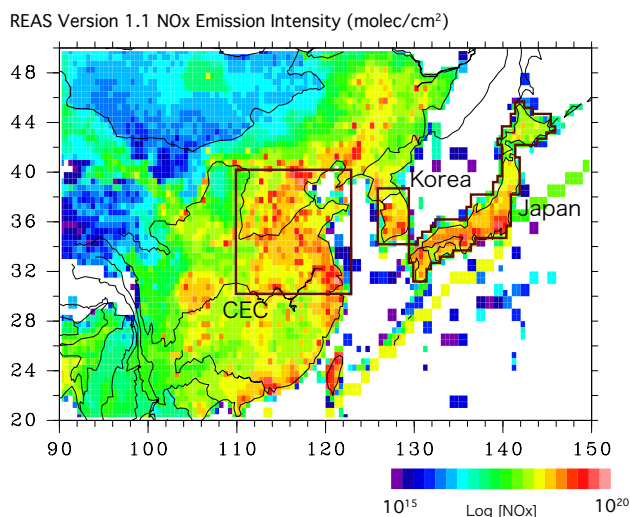


**Fig. 1.** Horizontal distribution of REAS NO<sub>x</sub> emission for year 2000. Square regions are average areas used for detailed analyses.

measurements (Irie et al., 2005). Quite similar results were also recently reported as results of a study including both GOME and SCanning Imaging Absorption spectrometer for Atmospheric CHartographyY (SCIAMACHY) data in a statistical analysis by van der A et al. (2006). However, as discussed by Richter et al. (2005) and van Noije et al. (2006), the GOME retrieval is very sensitive to several factors including cloud screening and other chemical/meteorological conditions. Systematic comparison of satellite NO<sub>2</sub> VCDs and application of the chemical transport model (CTM) plays an important role for emission analysis to overcome such difficulties. van Noije et al. (2006) presented a systematic comparison of NO<sub>2</sub> columns from 17 global CTMs and three state-of-the-art GOME retrievals for the year 2000. They report that, on average, the models underestimate the retrievals in industrial regions such as Europe, the eastern United States, and eastern China. They concluded that top-down estimations of NO<sub>x</sub> emissions from satellite retrieval are strongly dependent on the choice of model and retrieval. These results are based on global CTMs with coarse horizontal resolution, whereas a regional CTM can have much finer resolution, which is suitable for the resolution of recent emission inventories. As an example of a regional CTM application, Ma et al. (2006) compared the GOME-NO<sub>2</sub> VCDs with MM5/RADM regional model simulations for July 1996 and 2000 based on the emission inventory of Streets et al. (2003) for the year 2000 and the Chinese Ozone Research Programme (CORP) emission estimates for the year 1995 and questioned the accuracy of emission inventories. However, their studies are restricted to July of those two years; no inter-annual variation is discussed.

The GOME retrieval (top-down approach) provides long-term data for almost 7 years (January 1996–June 2003) and

CTM studies corresponding to that period with year-by-year emission estimates are absolutely necessary as a bottom-up analysis. GOME data can provide constraints for the inverse method of emission estimates (e.g., Martin et al., 2003; Jaeglé et al., 2005). They also provide recent emission trends, but such a long-term CTM study has not yet been reported for Asia. As successful applications for Asian air quality studies, the community multi-scale air quality model (CMAQ; Byun and Ching, 1999) has been used intensively by Zhang et al. (2002), Uno et al. (2005), Tanimoto et al. (2005), and Yamaji et al. (2006a). Herein, we report the results of systematic analyses of seasonal and interannual variations of NO<sub>2</sub> VCDs based on GOME data and the regional scale CTM, CMAQ, and sensitivity experiments with the latest emission inventory in Asia from 1996 to 2003.

## 2 Outline of CMAQ simulation, Emission Inventory and GOME retrieval

In the following, we will briefly describe the regional chemical transport model, the emission inventory, the GOME NO<sub>2</sub> retrievals and the settings used in the numerical experiments in this paper.

### (a) Chemical Transport Model, CMAQ

The three-dimensional regional-scale CTM used in this study was developed jointly by Kyushu University and the National Institute for Environmental Studies (Uno et al., 2005) based on the Models-3 CMAQ (ver. 4.4) modeling system released by the US EPA (Byun and Ching, 1999). Briefly, the model is driven by meteorological fields generated by the Regional Atmospheric Modeling System (RAMS; Pielke et al., 1992) with initial and boundary conditions defined by NCEP reanalysis data (2.5° resolution and 6 h interval). The horizontal model domain for the CMAQ simulation is 6240×5440 km<sup>2</sup> on a rotated polar stereographic map projection centered at 25° N, 115° E with 80×80 km<sup>2</sup> grid resolution (see Fig. 1 of Tanimoto et al., 2005). For vertical resolution, 14 layers are used in the sigma-z coordinate system up to 23 km, with about seven layers within the boundary layer below 2 km. The SAPRC-99 scheme (Carter et al., 2000) is applied for gas-phase chemistry (with a number of 72 chemical species and 214 chemical reactions, including 30 photochemical reactions), and the AERO3 module for aerosol calculation.

### (b) REAS emission inventory

Reliable emission inventories of air pollutants are becoming increasingly important to assess heavy air pollution problems in Asia. An emission inventory in Asia was reported for the TRACE-P and ACE-Asia field study by Streets et al. (2003) with 1°×1° resolution. A similar global emission inventory is provided in the EDGAR database (Olivier

et al., 2002). Recently, the Regional Emission inventory in Asia (REAS; Ohara et al., 2007<sup>1</sup>; Akimoto et al., 2006; Yamaji, 2006b) was constructed based on energy data, emissions factors, and other socio-economic information between the years 1980 and 2003. It provides an Asian emission inventory for ten chemical species: NO<sub>x</sub>, SO<sub>2</sub>, CO, CO<sub>2</sub>, nitrous oxide (N<sub>2</sub>O), NH<sub>3</sub>, black carbon (BC), organic carbon (OC), methane (CH<sub>4</sub>), and non-methane volatile organic compounds (NMVOC) from anthropogenic sources (combustion, non-combustion, agriculture, and others). All emission species from each source sector have been estimated based on activity data on the district levels for Japan, China, India, South Korea, Thailand and Pakistan. For those other countries, estimations are based on activity data of the national level. The emissions estimated for district and country level were distributed into a 0.5° × 0.5° grid using index data bases of population, location of large point source (LPS), road networks, and land coverage information.

REAS NO<sub>x</sub> emission inventories considered the fossil fuel (by assuming the initial ratio of NO:NO<sub>2</sub> = 9:1) and bio-fuel combustion, biomass burning and soil. REAS Soil NO<sub>x</sub> emission (sum of N-fertilized soil and natural soil) is estimated to be 400–500 GgN yr<sup>-1</sup> from China, which is approximately 12–15% of combustion base NO<sub>x</sub>. Present calculations do not include the lightning-related NO<sub>x</sub> emission because their contribution might be small in north east Asia region as discussed in Sect. 3.1. Another reason for excluding soil NO<sub>x</sub> and lightning-related NO<sub>x</sub> from the CMAQ simulation is that both of them are highly uncertain.

The NO<sub>x</sub> emission intensity (combustion base) of REAS version 1.1 for 2000 was estimated as 11.2 Tg-NO<sub>2</sub> yr<sup>-1</sup> for all of China (27.3 Tg-NO<sub>2</sub> for Asia). A similar number of 10.5 Tg-NO<sub>2</sub> yr<sup>-1</sup> was reported from TRACE-P (Streets et al., 2003), and 13.8 Tg-NO<sub>2</sub> yr<sup>-1</sup> from EDGAR ver. 3.2.

Figure 1 presents the horizontal distribution of REAS NO<sub>x</sub> emissions for 2000 using log-scale coloring. Figure 1 shows that large NO<sub>x</sub> emission regions are located in China (especially Hong-Kong, Shanghai, the North China Plain, and Beijing), Seoul, Pusan, Taiwan, and central and western parts of Japan. The horizontal distribution and location of hot spots are very similar to those shown by TRACE-P emission inventory by Streets et al. (2003). The square region is CEC, and REAS NO<sub>x</sub> emission within the CEC region are estimated at 4.86 Tg-NO<sub>2</sub> yr<sup>-1</sup>, which corresponds to 43% of the total NO<sub>x</sub> emission in China.

### (c) GOME Tropospheric NO<sub>2</sub> Vertical Column Densities (VCDs)

GOME is a passive remote sensing instrument on board the ERS-2 satellite launched in April 1995. The GOME instru-

<sup>1</sup>Ohara, T., Akimoto, H., Kurokawa, J., Horii, N., Yamaji, K., Yan, X., and Hayasaka, T.: REAS: Asian emission inventory for anthropogenic emission sources during the period 1980–2020, Atmos. Chem. Phys. Discuss., submitted, 2007.

ment observes the atmosphere at 10:30 local time (LT) and global coverage is achieved every 3 days with a footprint of 40 km latitude by 320 km longitude. For this study, we use the most recent version (ver. 2) of tropospheric NO<sub>2</sub> column data products retrieved by the University of Bremen (Richter et al., 2005). The retrieval version 2 data is based on 3-D CTM, SLIMCAT data, to exclude the stratospheric NO<sub>2</sub> contribution, monthly AMF (air mass factor) evaluated with NO<sub>2</sub> profiles from a run of the global model MOZART-2 for 1997.

This version 2 retrieval accounts for aerosol based on three different scenarios taken from the LOWTRAN database (marine, rural and urban) distributed according to surface type and CO<sub>2</sub> emissions. Surface reflectivity climatological data from Koelemeijer et al. (2003) are used. Details of cloud treatment have already been described by Richter et al. (2005). Briefly, the cloud screening used for this study is based on the FRESCO algorithm, which provides effective cloud fractionation. Snow-covered areas are flagged as cloudy and are therefore excluded from analysis. Aerosols are retrieved as thin clouds, and a very thick aerosol is also flagged as cloudy. Different from other retrievals, the remaining cloud fraction (cloud cover < 0.2) is not corrected in the GOME NO<sub>2</sub> retrieval of the University of Bremen. Therefore, for a situation in which all NO<sub>2</sub> are below the clouds, errors of up to 35% can occur (see Richter and Burrows, 2000). It does not include the effect of Asian dust or any seasonal variability. Furthermore, no trend in aerosol is assumed. An increase in non absorbing aerosols (e.g. sulfate) might result in higher sensitivity of GOME to NO<sub>2</sub> within and above the aerosol layers, possibly enhancing the observed trend (Richter et al., 2005; van der A et al., 2006; Martin et al., 2003). The intercomparison by van Noije et al. (2006) reported that the GOME NO<sub>2</sub> retrieval by the University of Bremen gives a slightly higher value over the Chinese winter (for 2000) when compared with two other retrievals (BIRA/KNMI and Dalhousie/SAO).

A rough estimate of the GOME NO<sub>2</sub> errors is an additive error of 0.5–1.0 × 10<sup>15</sup> molecule cm<sup>-2</sup> and a relative error of 40–60% over polluted areas. In addition, the uncertainty for the annual average is approximately 15% (e.g. Richter et al., 2005).

For this study, the GOME tropospheric NO<sub>2</sub> swath data (ver. 2) files giving the location and value for each measurement pixel are all interpolated into a 0.5° × 0.5° longitude-latitude map (as with the REAS grid resolution). The GOME tropospheric NO<sub>2</sub> data for the period of January 1996–June 2003 are used in this study.

### (d) Setting of numerical experiments by CMAQ/REAS

In this study, an eight-full-year simulation was conducted for 1996–2003. For this CMAQ modeling system, all emissions were obtained from 0.5° × 0.5° resolution of the REAS ver. 1.1 database. The effect of seasonal dependence of emissions were examined by Streets et al. (2003), and they

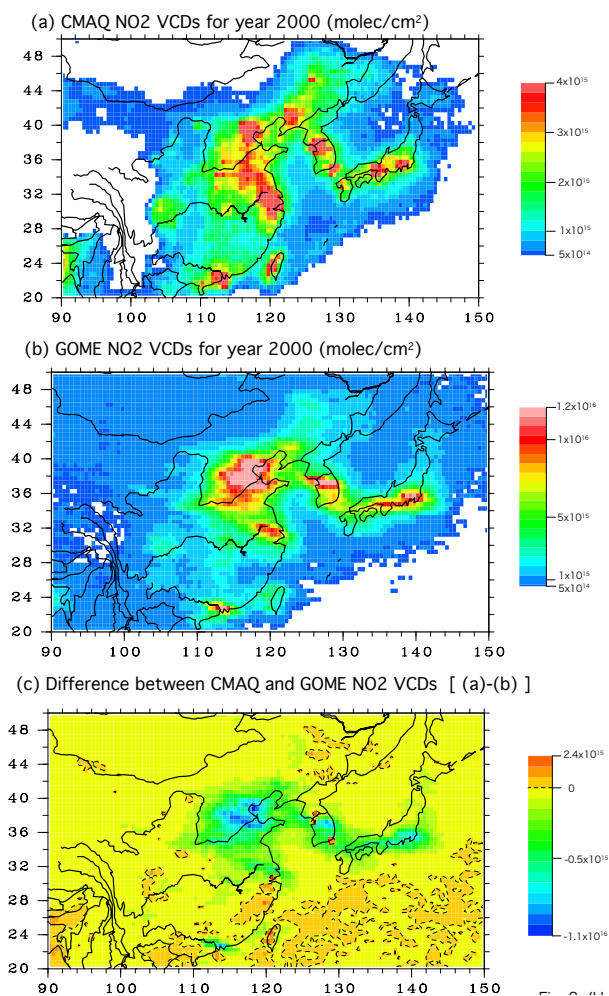


**Fig. 2.** Annual mean CMAQ simulated tropospheric NO<sub>2</sub> VCDs averaged by SRA for year 2000, (b) Annual mean GOME satellite data for year 2000 and (c) the difference of CMAQ and GOME [(a)–(b)].

indicated that domestic space-heating component has a seasonality and the ratio of monthly emissions was approximately 1.2 between maxima and minima (see Fig. 7 of Streets et al., 2003). However, the specification of emission seasonality is very difficult, so emission intensity for the CMAQ is set as constant for each year and no seasonal variation is assumed. The initial fields and monthly averaged lateral boundary condition for most chemical tracers are provided from a global chemical transport model (CHASER; Sudo et al., 2002). This fixed lateral boundary condition is used for the eight-full-year simulation (i.e., no interannual variation of lateral conditions is assumed). The CMAQ output data are all interpolated to  $0.5^\circ \times 0.5^\circ$  resolution of REAS to facilitate an easy comparison.

Two sets of numerical experiments were conducted. Series E00Myy simulations used the fixed emission for 2000 with year-by-year meteorology. Series EyyMyy use both

year-by-year emissions and meteorology. These two experiments were set to elucidate the sensitivity for both meteorology and changes in emission intensity. The GOME measurements in low latitudes and middle latitudes are always taken at the same LT (approximately 10:30 LT). Therefore, we used the CMAQ output of 03:00 UTC (11:00 LT for China and 12:00 LT for Japan) for comparison.

### 3 Results and discussion

#### 3.1 General distribution and comparison of NO<sub>2</sub> in Asia for 2000

We will show a general comparison of CMAQ NO<sub>2</sub> VCDs and GOME retrieval results. To obtain the CMAQ simulated tropospheric NO<sub>2</sub> VCDs, we integrated the column NO<sub>2</sub> loading from surface to 10 km height. No seasonal variation of tropopause height is considered because approximately 95% of NO<sub>2</sub> resides at heights below 3 km in the CMAQ simulation and the same lateral boundary condition is used for all model experiments. We set three regions in central east China (CEC; 30° N, 110° E to 40° N, 123° E), Korea and Japan to produce detailed comparisons (see Fig. 1). The definition of CEC is the same area used by Richter et al. (2005). Please note that we are excluding lightning NO<sub>x</sub> sources from the CMAQ, which introduces a downward bias in the vertical profiles from CMAQ. However, the absolute amount of NO<sub>x</sub> emissions of lightning, the fact that the GOME overpass is at the diurnal minimum of lightning activity, and the much smaller NO<sub>2</sub>/NO<sub>x</sub> ratio at high altitudes all combine to render the lightning signal in the satellite data as small. Furthermore, according to results by Boersma et al. (2005, Fig. 5), the contribution of lightning NO<sub>2</sub> is small for the CEC region (less than  $0.05 \times 10^{15}$  mol/cm<sup>2</sup>/year), but the GOME and CMAQ results are more than two orders of magnitude larger. We believe that the effect of lightning over the China-Korea-Japan region will be much smaller than the anthropogenic emission of NO<sub>x</sub>.

The GOME observations are only taken every 3 days. To make a systematic comparison, we defined two averaging methods for the regions of interest. Satellite Region Average (SRA) is the average of CMAQ NO<sub>2</sub> VCDs for exactly the same timing and grid point as the GOME observation, which is most suitable for comparison with satellite data. Another average is the simple region average without any consideration of GOME observation timing; this we call as the simple CTM Region Average (CRA). The difference between SRA and CRA gives an indication on the observation bias of GOME retrievals as result of the measurement sampling and cloud selection.

Figure 2 shows (a) the annual mean CMAQ simulated tropospheric NO<sub>2</sub> VCDs averaged by SRA for year the 2000, (b) the annual mean GOME satellite data for the year 2000, and (c) the difference of CMAQ and GOME [(a)–(b)].

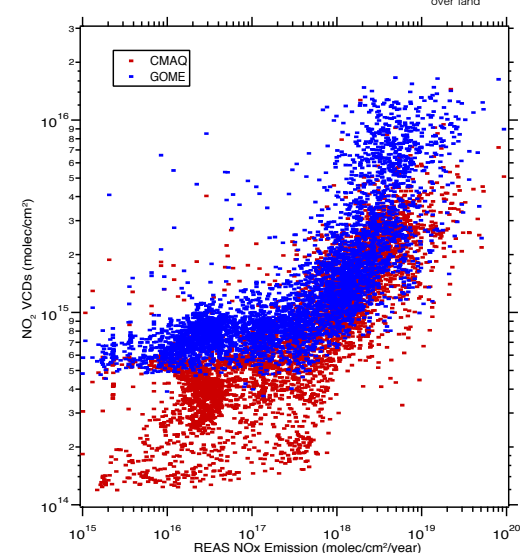
Figure 3 shows (a) scatter plots between REAS NO<sub>x</sub> emission and NO<sub>2</sub> VCDs of CMAQ and GOME excluding the ocean area, and (b) scatter plots between CMAQ NO<sub>2</sub> VCDs and GOME retrieval for all grid points.

The NO<sub>2</sub> chemical reactions are calculated using the SAPRC-99 chemical reaction scheme (already written in Sect. 2a). Based on the calculation result for the year 2000, we evaluated the time-spatial distribution of NO<sub>2</sub>. CMAQ simulated NO<sub>2</sub> VCDs (Fig. 2a) shows a quite similar distribution with the REAS NO<sub>x</sub> emission map (Fig. 1). Annual mean GOME NO<sub>2</sub> VCDs (shown in Fig. 2b) and the difference to the CMAQ NO<sub>2</sub> VCDs (Fig. 2c) provide important information related to Asian NO<sub>x</sub> emissions. High GOME NO<sub>2</sub> VCDs regions generally agree with the CMAQ (and REAS) results. The difference between CMAQ and GOME (Fig. 2c) indicates that the CMAQ results underestimate the GOME retrievals over polluted industrial regions such as CEC, a major part of Korea, Hong-Kong, and central and western Japan. It is noteworthy that CMAQ shows a high concentration over Taiwan, two large cities in Korea (Seoul and Pusan) and northeastern China (e.g., the region between Shenyang and Changchun), which are not strongly identified in GOME data mainly due to the strong longitudinal averaging of GOME data. A more detailed analysis of the NO<sub>x</sub> emissions, GOME retrieval and CMAQ NO<sub>2</sub> is presented in Fig. 3. Figure 3a shows the relationship between REAS NO<sub>x</sub> emission (assuming NO:NO<sub>2</sub>=9:1 and converted to molecule cm<sup>-2</sup>) and NO<sub>2</sub> VCDs over the land surface, respectively, by GOME (blue) and CMAQ (red). The GOME NO<sub>2</sub> value has a clear cut-off at the level of  $0.5 \times 10^{15}$  molecule cm<sup>-2</sup>. This figure indicates the responses of emission to the atmospheric concentrations for the model and GOME. The data points are scattered widely. Nevertheless, the nearly linear relationship that was expected is apparent between NO<sub>x</sub> emission and NO<sub>2</sub> concentration.

Finally, Fig. 3b shows the systematic under-estimation of CMAQ NO<sub>2</sub> for all grid points. Most CMAQ NO<sub>2</sub> VCDs are distributed between  $y=x$  and  $y=3x$  (i.e. factor 3 range). The red squares indicate grid points within the CEC region, blue triangles are used for Korea, green squares for Japan, and yellow dots for data from west of 105° E. All other data are shown as gray dots. As this figure shows, most Japanese data are located around the line between  $y=x$  and  $y=3x$ , which is a fundamentally identical pattern to that obtained using CEC data (even if some CEC data are located near the  $y=4x$  line), whereas most Korean data are located between  $y=2x$  and  $y=3x$ . The GOME retrieval provides NO<sub>2</sub> VCDs, which are the result of the actual NO<sub>x</sub> emissions and which are independent of a priori assumptions of their magnitude and distribution. Systematic differences from CMAQ-simulated NO<sub>2</sub> show that emission data require some re-examination. The possible factors are, for example, the basic energy consumption, emission factors, and socio-economic data used for construction of the emission inventory.

For the low emission region (intensity below

(a) Scatter of REAS NO<sub>x</sub> Emission and (CMAQ and GOME NO<sub>2</sub> VCDs)<sub>over land</sub>



(b) Scatter of CMAQ and GOME NO<sub>2</sub> VCDs

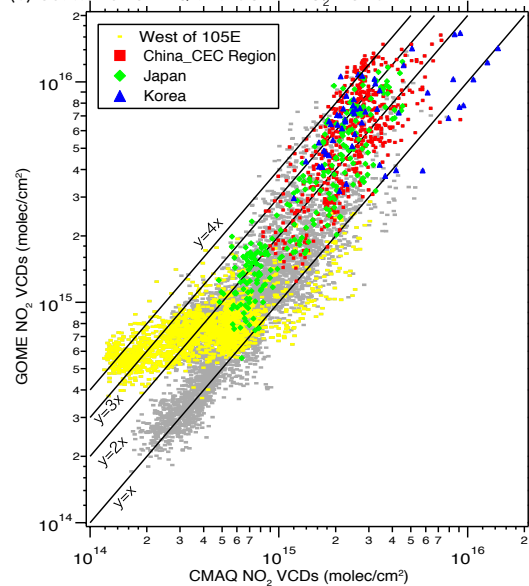


**Fig. 3.** Scatter plots between REAS NO<sub>x</sub> emission and NO<sub>2</sub> VCDs excluding the ocean area for the year 2000 and (b) scatter plots between annual averaged CMAQ NO<sub>2</sub> VCDs and GOME retrieval for all grid points (shown by grey points except for the points indicated in the figure).

$10^{17}$  molecule cm<sup>-2</sup>) shown in Fig. 3a, GOME and CMAQ responses are different: GOME is systematically higher than CMAQ. This is mainly attributable to the effect of biomass burning. The contribution of biomass burning NO<sub>2</sub> is higher in these regions, whereas the REAS emission inventory for biomass burning is taken from TRACE-P emission inventory and is different for 2000. An almost identical result is pointed out by Ma et al. (2006). It is also important to point out that the gray dot points below



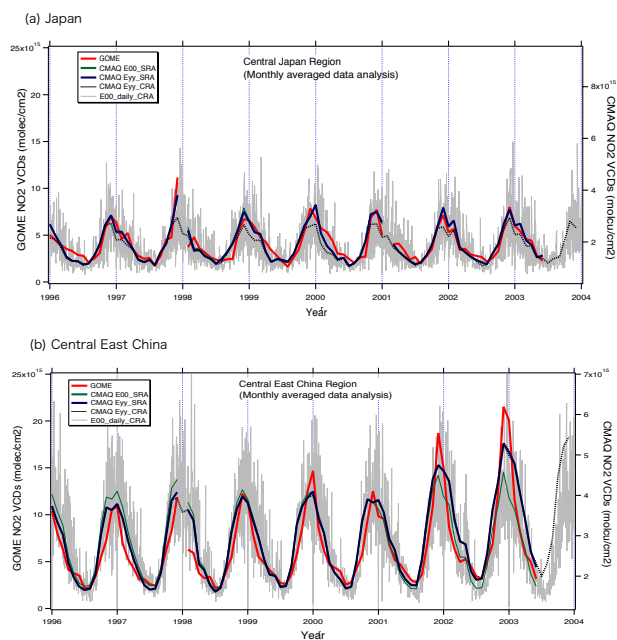


**Fig. 4.** Evolution of the tropospheric columns of NO<sub>2</sub> over the region of (a) Japan and (b) CEC. The thick red line represents the monthly averaged GOME NO<sub>2</sub> VCDs, and thick-green line is CMAQ E00Myy\_SRA, thick-black dotted line is EyyMyy\_SRA and thin-dashed-black line is EyyMyy\_CRA. The gray vertical line shows the daily averaged value from CMAQ E00Myy\_CRA. (SRA is the Satellite Region Average, and CRA is the simple CTM Region Average. E00Myy simulation used the fixed emission for 2000 with year by year meteorology, and EyyMyy use both year-by-year emission and meteorology).

$0.6 \times 10^{15}$  molecule cm<sup>-2</sup> (shown in Fig. 3b) are mainly over the ocean and show an almost 1:1 relationship between GOME and CMAQ VCDs. Finally, we have to point out that for the region west of 105° E (as indicated in Fig. 3b), the contribution of soil NO<sub>x</sub> over the combustion-based NO<sub>x</sub> is 5% (winter) – 44% (summer). For that reason, soil NO<sub>x</sub> emissions might be important for these regions in summer.

### 3.2 Analysis of interannual and seasonal variations of NO<sub>2</sub>

The evolution of the tropospheric columns of NO<sub>2</sub> above the regions of Japan and CEC (see in Fig. 1) are shown in Fig. 4. The thick red line represents the monthly averaged GOME NO<sub>2</sub> VCDs. The figure also includes results of CMAQ E00Myy\_SRA (thick-green), EyyMyy\_SRA (thick-black dotted line), and EyyMyy\_CRA (thin-dashed-black line). The gray vertical line is the daily averaged value from E00Myy\_CRA in order to show the range of day-by-day variation of simulated concentration. GOME and SRA average data are only shown until June 2003 because of data availability. Because the CMAQ underestimates the GOME retrieval, the vertical axis for CMAQ (right axis) is adjusted to improve the view.

First, for the Japan region (Fig. 4a), GOME retrieval and CMAQ EyyMyy\_SRA show good agreement and no clear increase, which is consistent with the REAS emission inventory for Japan that shows no clear increasing trend (the REAS variation is less than ±2% during 1996–2003). The best fitting lines based on all data for SRA and CRA are

SRA:  $\text{GOME\_NO}_2 = -5.55\text{E}14 + 2.41 \times \text{CMAQ\_NO}_2$  (molecule cm<sup>-2</sup>) ( $R=0.919$ ).

CRA:  $\text{GOME\_NO}_2 = -1.26\text{E}15 + 2.98 \times \text{CMAQ\_NO}_2$  (molecule cm<sup>-2</sup>) ( $R=0.878$ ).

The CMAQ values are approximately 40% that of GOME. Data for February 2001 are not used because only one observation day was available. The SRA averaging method extracts the CMAQ results for the clear fine weather condition (i.e. less cloudy) that is favorable for high concentration conditions, whereas the CRA extracts all weather conditions, including the strong wind condition (which yields a smaller regression coefficient). The exact reason why the CMAQ underestimates the GOME VCDs remains unclear; however, the high correlation supports that the combination of CMAQ and GOME results is suitable for analysis of the interannual and seasonal variation of NO<sub>2</sub> concentration and emission trends.

The monthly means of GOME and CMAQ EyyMyy\_SRA are located within the daily variation line of E00Myy\_CRA, meaning that the emission trend does not increase from the estimate for 2000. The CMAQ results reproduce the seasonal variation very well, showing the summer (July–August) minimum and winter (December) maximum. Some differences pertain between SRA and CRA results, especially in winter (CRA is smaller than SRA), which indicates the GOME retrieval has a slightly positive bias in Japan because of GOME's observation on days with clear weather and the small number of observations in winter.

The results for CEC (Fig. 4b) provide very important facts about China. First, the general agreement between GOME and CMAQ looks similar to Japan. It is important to point out that GOME retrieval shows a strongly increasing trend during 2001–2003, but its trend is gentler during 1996 and 1999. For China, the result of EyyMyy\_SRA and EyyMyy\_CRA is almost identical, which is a result of the choice of a wide averaging region (approximately 1000 × 1000 km<sup>2</sup>). Consequently, the monthly CRA result is also suitable for comparison with monthly mean GOME data for a wide region like CEC. It is also worth noting that averaging should minimize pure statistical effects, but systematic effects should remain. Particularly, the cloud filter for the GOME observations should have an influence.

Several sensitivity lines in Fig. 4b are very interesting. The CMAQ E00Myy\_SRA (fixed emission for 2000) basically retrieves the interannual variation of GOME, but shows relatively high values before 1998, and relatively smaller values after 2002. That fact indicates that the NO<sub>x</sub> emission is increasing year-by-year between 1996 and 2003, even considering the effect of meteorological variability. It is

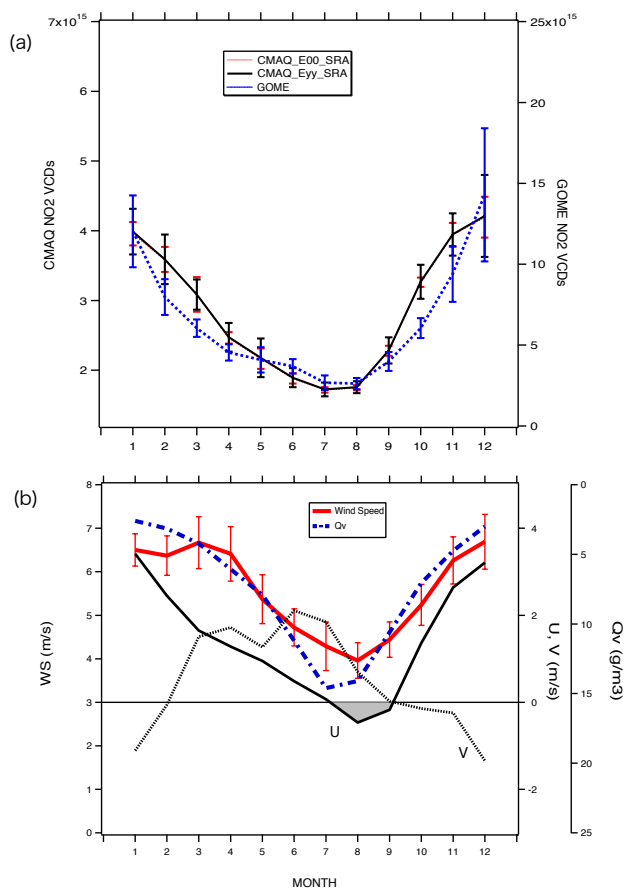


**Fig. 5.** Seasonal variation of NO<sub>2</sub> VCDs and meteorological parameters for CMAQ and GOME averaged by SRA over 7 years. Error bars show the range of plus and minus one-standard deviation. **(a)** NO<sub>2</sub> VCDs averaged over CEC and **(b)** the wind speed and water vapor mixing ratio ( $Q_v$ ) over CEC region from RAMS simulation. Wind speed and  $Q_v$  are the average values of the surface and  $z=500$  m.

interesting that the results of E00Myy show good agreement with GOME NO<sub>2</sub> during 1999 and 2001, suggesting that emission increases during this period are small or that the variation of meteorology masks the trend; additional relevant details will be discussed in Sect. 3.3. The CMAQ results for EyyMyy (SRA and CRA are almost the same) reproduce well the increasing trend of the GOME columns from 1996 and 2003, especially the increasing trend of the summer time minimum value. We can see that the winter peak value of CMAQ NO<sub>2</sub> during 2002–2003 is relatively smaller than that of GOME. The reason is unclear, but possible reasons will be addressed later in Sect. 3.3.

The seasonal variation in CEC is basically identical to that in Japan. Figure 5 shows seasonal variations of NO<sub>2</sub> VCDs for CMAQ and GOME. Here, seven-year averaged data for SRA are used for GOME and CMAQ NO<sub>2</sub> VCDs; the vertical axis is different for CMAQ and GOME. Error bars show

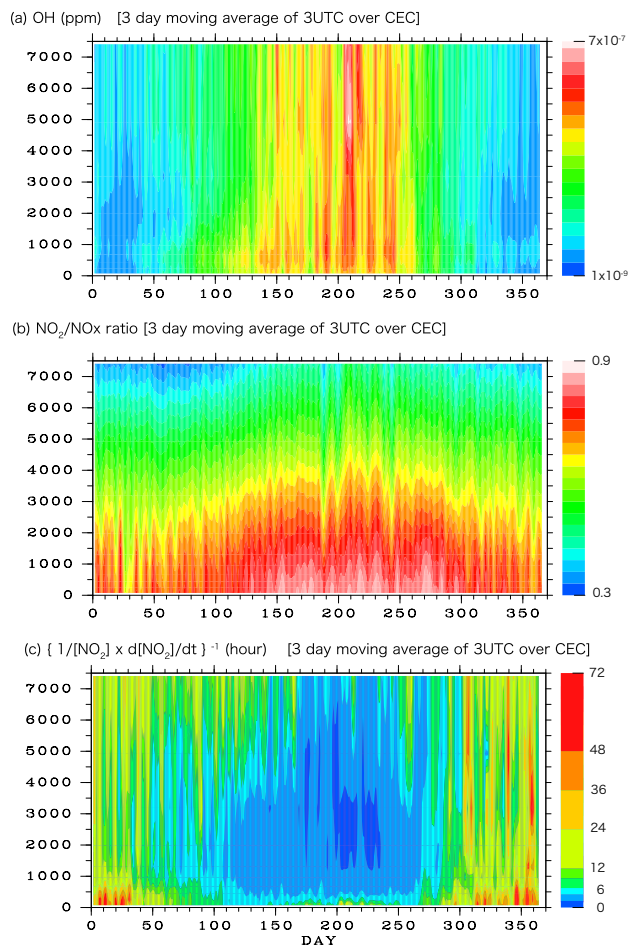


**Fig. 6.** CEC region 3-day moving average (at 03:00 UTC) of **(a)** the time-height cross section of OH radical concentration (ppm), **(b)** the NO<sub>2</sub>/NO<sub>x</sub> ratio and **(c)** the NO<sub>2</sub> “chemical lifetime”, as evaluated by  $\{1/[\text{NO}_2] \times d[\text{NO}_2]/dt\}^{-1}$  (hour) only from the chemical reaction term.

the range from one standard deviation more to one less. The figure also shows the wind speed and water vapor mixing ratio,  $Q_v$  over the CEC region from RAMS simulation. Wind speed and  $Q_v$  quantities are the respective averages of values at the surface and those at  $z=500$  m.

Figure 6 shows the CEC region 3-day moving average (at 03:00 UTC) of **(a)** the time-height cross section of OH radical concentration, **(b)** the NO<sub>2</sub>/NO<sub>x</sub> ratio, and **(c)** the NO<sub>2</sub> “chemical lifetime”, as evaluated by  $\{1/[\text{NO}_2] \times d[\text{NO}_2]/dt\}^{-1}$  (hour) solely from the chemical reaction term. The OH concentrations are higher at high altitudes, especially during summer. This is an important factor determining the short lifetime of NO<sub>2</sub> during summer. Furthermore, winds at higher altitudes (not shown) are usually stronger and produce a large advection out of the source region. These effects tend to reduce the NO<sub>2</sub> lifetime. For the NO and NO<sub>2</sub> ratio, we assume that NO:NO<sub>2</sub> = 9:1 from emission sources.

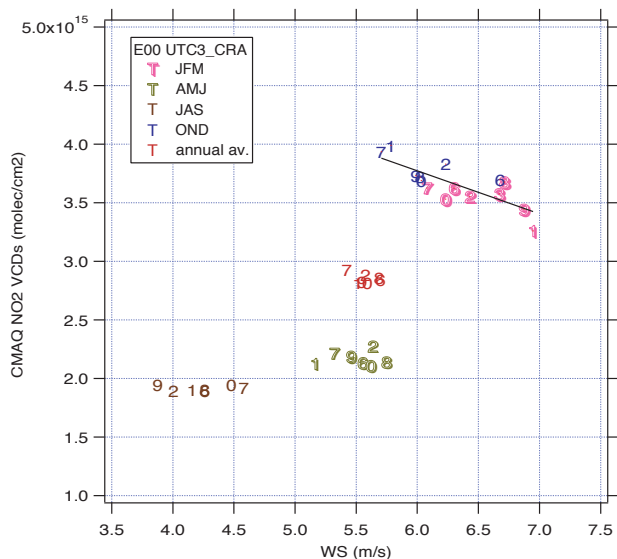


**Fig. 7.** Scatter plot of three-month averaged NO<sub>2</sub> VCDs and wind speed in the CEC region during 1996 and 2003. Colors represent the averaging duration (red is the annual average) and numbers show the last digit of the year (e.g., 9=1999 and 1=2001).

However, the chemical conversion speed from NO to NO<sub>2</sub> is high. The model simulated NO<sub>2</sub>/NO<sub>x</sub> ratio over the CEC (averaged below  $z=500$  m) is 0.68 (in winter) – 0.85 (in summer). The chemical lifetime of NO<sub>2</sub> is very important. The chemical decay rate of NO<sub>2</sub> is evaluated as

$$\tau = \left( \frac{1}{[NO_2]} \frac{d[NO_2]}{dt} \right)_{\text{chemical reaction}}^{-1}$$

That equation clearly shows the summer minimum of 2–3 h and a winter maximum of 36–72 h (or more; see Fig. 6c).

Maximum values of the NO<sub>2</sub> columns occur in December even though the wind speed is higher. This indicates that the effect of the longer chemical lifetime of NO<sub>2</sub> is more important than that of strong wind. While the minimum value is observed in July and August because of the strong vertical mixing, the short lifetime of NO<sub>2</sub> and the inflow of moist air from the Pacific Ocean side. At this minimum value, CMAQ VCDs corresponds to 64% of the value of GOME VCDs. This seasonal variation is asymmetric and the slope (curvature) of the seasonal variation of NO<sub>2</sub> both for CMAQ and GOME is different during January–June and September–December. For this seasonal variation of NO<sub>2</sub>, wind changes must play an important role; the variation of NO<sub>2</sub> and the east wind (U component) are well correlated. Because the east wind indicates the summer monsoon from the Pacific Ocean side and will bring fresh & moist air, as indicated from the increase of  $Q_v$ . This east wind ceases in September (rapid stop of summer monsoon) and changes to the west and north wind directions resulting in a rapid increase of NO<sub>2</sub> levels.

Both CMAQ and GOME data show a large standard deviation during January–March and October–December, which shows that the variability of meteorology plays an important role in these seasons. When comparing the scaled GOME and model NO<sub>2</sub> variation, GOME retrievals during February–April and September–November shows larger dips (concave shape) than CMAQ, even when considering the error bar of the standard deviation. The exact reasons for this discrepancy are not yet clear and need more work both from the CTM side and satellite retrieval method.

### 3.3 Role of interannual variability of wind speed and analysis of recent trends of emission intensity

The effect of interannual variability of meteorology (especially wind speed) plays an important role in determining the NO<sub>2</sub> concentration level. Sensitivity experiments with fixed emission rate for 2000 (E00My) provide the effect of wind speed for NO<sub>2</sub> concentration.

Figure 7 shows a scatter plot of three-month averaged CMAQ NO<sub>2</sub> VCDs and wind speed in the CEC region during 1996 and 2003. Wind speed below  $z=500$  m is averaged in the figure. Three months averaged and annual averaged value are shown in different color and numbers show the last digit of the year (e.g., 9=1999 and 1=2001). This analysis is important to show the effect of wind speed variability for the concentration level to analyze the GOME retrieval (i.e., observed data includes the effect of meteorological variability).

The figure shows that NO<sub>2</sub> VCDs are higher in winter (JFM) and fall (OND). It is noteworthy that 1999 and 2001 in JFM have higher wind speeds. Furthermore, 1997 and 2000 in JFM have slower overall wind speeds and the difference is about 0.7–1.0 m s<sup>-1</sup> (corresponding to 15% of magnitude). The difference of NO<sub>2</sub> VCDs in 1997 and 2001 exceeded 0.3–0.4 molecule cm<sup>-2</sup> (10%) compared to 1999 and 2001. The linear fitting result for OND and JFM is

$$\text{CMAQ\_NO}_2 \text{ (molecule cm}^{-2}\text{)} = 5.976\text{E}15 - 3.671\text{E}14 \times \text{WS (m s}^{-1}\text{)} \quad (R=-0.784).$$

That result implies that the 10% difference in WS (around WS=6.5 m s<sup>-1</sup>) causes a 10% difference in NO<sub>2</sub> VCDs. The detection of an emission trend from satellite (and/or surface monitoring stations) in fall or winter therefore results in a larger error because of the variability of meteorology.

For spring and summer seasons, NO<sub>2</sub> VCDs are smaller (40–50% of that of OND) and are not strongly sensitive to the change of wind speed (for AMJ, CMAQ NO<sub>2</sub> ranges 2.11–2.27E15 molecule·cm<sup>-2</sup> (approximately 7%). This characteristic is also valid for annual averages (ranges 2.82–2.92 molecule cm<sup>-2</sup>; approximately 3.5%). We conclude that the analysis of summer time and annual average NO<sub>2</sub> VCDs is much less sensitive to variability of meteorology and is suitable for the analysis of emission trends, even though it still includes the 3–7% variation arising from meteorological variability.



Another important analysis is the recent emission increase in CEC. The best fit between GOME and CMAQ (EyyMyy\_SRA) for CEC (for the plot shown in Fig. 4) is

$$\text{CMAQ\_NO}_2 = 5.12\text{E}15 - 5.00\text{E}15 \times \exp[-1.45\text{E}-16 \times \text{GOME\_NO}_2]$$

This exponential fit indicates that GOME NO<sub>2</sub> is more enhanced when the CMAQ NO<sub>2</sub> concentration becomes higher (i.e., emission becomes higher); most of these conditions occur after the year 2000.

The exact reason why the relationship between CMAQ NO<sub>2</sub> and GOME NO<sub>2</sub> becomes nonlinear remains unclear. However, several possible reasons include: (1) the estimated emissions do not reflect the recent NO<sub>x</sub> emission increases enough, and (2) the basic assumptions (e.g., no aerosol trend or change in air mass factor, etc.) of GOME NO<sub>2</sub> retrieval require re-consideration. The assumption of no trend in aerosols might not be appropriate in China. The REAS SO<sub>2</sub> emission in China increases by about 30% between the year 2000–2003, which results in a CMAQ sulfate increase of 13% in CEC region. Based on CMAQ calculations over the CEC region (below  $z=500$  m), the region-averaged annual mean sulfate aerosol dominates 54.6% ( $11.1 \mu\text{g}/\text{m}^3$ ) of the total aerosol mass concentration. The respective fractions of nitrate, black carbon, and organic carbon to total aerosol are 25.3%, 5.3%, and 14.8%. Therefore, we believe that the main aerosol load in China is sulfate aerosol. Furthermore, REAS emission estimates for black carbon (BC) and organic carbon (OC) respectively show only 4% and 2% increases during 2000–2003, which are attributable to decreased bio-fuel emissions in China. The effect of increased aerosol absorption must be less than that of sulfate. However, detailed studies are necessary to better understand differences in recent NO<sub>2</sub> trends between CMAQ and GOME.

Our final and strongest interest is the understanding of the recent trend of emission increases in CEC. Figure 8 shows the trend of GOME NO<sub>2</sub>, CMAQ NO<sub>2</sub> and REAS NO<sub>x</sub> emission normalized to 2000. To determine the annual average of GOME for 1998, the January 1997 value was used in place of the missing observation of January 1998. The dashed line with an open black circle shows the variation of E00Myy simulation (0.99–1.03), which shows the effect of meteorological variability. The normalized result for CMAQ and REAS shows a very similar trend, indicating that CMAQ NO<sub>2</sub> VCDs responds to the NO<sub>x</sub> emission trend with almost equivalent magnitude. A similar response for the MOZART model is also discussed in Richter et al. (2005).

As depicted in Fig. 7, GOME NO<sub>2</sub> is sensitive to the selection of season, so three cases of average (simple annual average, average between May and October and between July and September (JAS)) are plotted. The green vertical bar shows the range of variation caused by the choice of averaging period of GOME; the error bar has an order of 5–10%. An increasing trend of 1996–1998 and 2000–2002 for GOME and CMAQ/REAS shows a good agreement, even though the GOME data give a slightly steeper trend after the

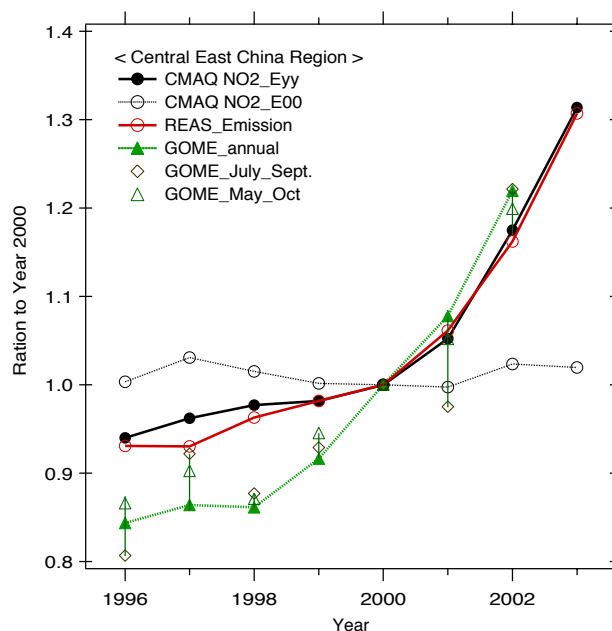


**Fig. 8.** Trend of GOME NO<sub>2</sub>, CMAQ NO<sub>2</sub> and REAS NO<sub>x</sub> emission normalized at 2000. The dashed line with an open circle shows variation of the E00Myy simulation.

year 2000 (GOME is approximately 10–11% yr<sup>-1</sup>, whereas CMAQ/REAS is 8–9% yr<sup>-1</sup>). The greatest difference also can be found between 1998 and 2000. The CMAQ/REAS result shows only a few percentage points of increase, but GOME gives more than 8% yr<sup>-1</sup> of increase. This 8%·yr<sup>-1</sup> increase exceeds the possible estimation error bar attributable to the meteorological variability (ca. 3–4%). Akimoto et al. (2006) and Zhang et al. (2007)<sup>2</sup> discussed the reliability of statistical reports from the Chinese government during this period. The most likely explanation is that the REAS emission trend (based on Chinese data) underestimates the rapid growth of emissions. This result highlights that combinations of CTM based on bottom-up inventories with satellite top-down estimates can play an important role in improving emission inventory estimates and provide very useful information that advances the development of a reliable CTM simulation.

#### 4 Conclusions

Systematic analyses of interannual and seasonal variations of tropospheric NO<sub>2</sub> vertical column densities (VCDs) based on GOME satellite data and the regional scale CTM, CMAQ, were presented over East Asia for the time period from January 1996 to June 2003. Numerical simulations with a year-

<sup>2</sup>Zhang, Q., Streets, D. G., He, K., Wang, Y., et al.: NO<sub>x</sub> emission trends for China, 1995–2004: The view from the ground and the view from space, *J. Geophys. Res.*, submitted, 2007.

by-year base of the REAS emission inventory in Asia during the same period were analyzed.

The main results are:

1. The horizontal distribution of annual averaged GOME NO<sub>2</sub> VCDs for 2000 generally agrees with CMAQ/REAS results. However, CMAQ results underestimate GOME retrievals by factors of 2–4 over polluted industrial regions such as Central East China (CEC), the major part of Korea, Hong-Kong, and central and western areas of Japan. Examination of differences of GOME and CMAQ also suggested that the emission inventory of some regions (e.g., Taiwan, two large city region of Korea and northeastern China) demand re-examination.
2. Evolution of the tropospheric columns of NO<sub>2</sub> above Japan and CEC between 1996 and 2003 was examined. For the Japan region, GOME retrieval and CMAQ NO<sub>2</sub> show a good agreement and no clear increasing trend, which is consistent with the REAS emission inventory for Japan. For CEC, the general agreement between GOME and CMAQ is also good. Both GOME and CMAQ NO<sub>2</sub> show a very sharp increasing trend after 2000. The seasonal cycle of NO<sub>2</sub> VCDs from both CMAQ and GOME is asymmetric.
3. A sensitivity experiment with a fixed emission rate for year 2000 shows that detection of emission trends over CEC from satellite data in fall or winter result in larger errors because of the variability of meteorology. Examination during summer and annual averaged NO<sub>2</sub> VCDs is much less sensitive to variability of meteorology and suitability of analysis of emission trends, even though it still includes 3–7% of the variability coming from meteorological variability.
4. Recent trends of annual emission increases in CEC were examined. Increasing trends of 1996–1998 and 2000–2002 for GOME and CMAQ/REAS shows a good agreement, but the increasing rate of the GOME data is approximately 10–11% yr<sup>-1</sup> after 2000, slightly steeper than CMAQ/REAS (8–9% yr<sup>-1</sup>). The greatest difference was found between the years 1998 and 2000. The CMAQ/REAS shows only a few percentage points of increase, while GOME gives more than 8% yr<sup>-1</sup> of increase. The exact reason remains unclear, but the most likely explanation is that the REAS emission trend (based on the Chinese statistics) underestimates the rapid growth of emissions during this time period.

*Acknowledgements.* This study was supported in part by funds from a Grant-in-Aid for Scientific Research under Grant No. 17360259 from the Ministry of Education, Culture, Sports, Science and Technology of Japan, and from the Steel Industry Foundation for the Advancement of Environmental Protection Technology (SEPT) and the European Union through ACCENT.

Edited by: T. Wagner

## References

- Akimoto, H., Ohara, T., Kurokawa, J., and Horii, N.: Verification of energy consumption in China during 1996–2003 by satellite observation, *Atmos. Environ.*, 40, 7663–7667, 2006.
- Boersma, K. F., Eskes, H. J., Meijer, E. W., and Kelder, H. M.: Estimates of lightning NO<sub>x</sub> production from GOME satellite observations, *Atmos. Chem. Phys.*, 5, 2311–2331, 2005, <http://www.atmos-chem-phys.net/5/2311/2005/>.
- Byun, D. W. and Ching, J. K. S. (Eds.): Science algorithms of the EPA Models-3 community multi-scale air quality (CMAQ) modeling system. *NERL*, Research Triangle Park, NC EPA/ 600/R-99/030, 1999.
- Carter, W. P. L.: Documentation of the SAPRC-99 chemical mechanism for VOC reactivity assessment, Final report to California Air Resource Board, Contract No. 92-329 and 95-308, May, 2000.
- Irie, H., Sudo, K., Akimoto, H., et al.: Evaluation of long-term tropospheric NO<sub>2</sub> data obtained by GOME over East Asia in 1996–2002, *Geophys. Res. Lett.*, 32, L11810, doi:10.1029/2005GL022770, 2005.
- Jaeglé, L., Steinberger, L., Martin, R. V., and Chance, K.: Global partitioning of NO<sub>x</sub> sources using satellite observations: Relative roles of fossil fuel combustion, biomass burning and soil emissions, *Faraday Discuss.*, 130, 407–423, 2005.
- Koelmeijer, R. B. A., de Haan, J. F., and Stammes, P.: A database of spectral surface reflectivity in the range 335–772 nm derived from 5.5 years of GOME observations, *J. Geophys. Res.*, 108(D2), 4070, doi:10.1029/2002JD002429, 2003.
- Ma, J., Richter, A., Burrows, J. P., Nüß, H., and van Aardenne, J. A.: Comparison of model-simulated tropospheric NO<sub>2</sub> over China with GOME-satellite data, *Atmos. Environ.*, 40, 593–604, 2006.
- Martin, R. V., Jacob, D. J., Chance, K., Kurosu, T. P., Palmer, P. I., and Evans, M. J.: Global inventory of nitrogen oxide emissions constrained by space-based observations of NO<sub>2</sub> columns, *J. Geophys. Res.*, 108, 4537, doi:10.1029/2003JD003453, 2003.
- Olivier, J. G. J., Berdowski, J. J. M., Peters, J. A. H. W., Visschedijk, A. J. H., Bekker, J., and Bloos, J. P. J.: Applications of EDGAR: Emission Database for Global Atmospheric Research. Dutch National Research Programme on Global Air Pollution and Climate Change, report no. 410 200 051, 2002.
- Pielke, R. A., Cotton, W. R., Walko, R. L., Tremback, C. J., Lyons, W. A., Grasso, L. D., Nicholls, M. E., Moran, M. D., Wesley, D. A., Lee, T. J., and Copeland, J. H.: A comprehensive meteorological modeling system—RAMS. *Meteorol. Atmos. Phys.*, 49, 69–91, 1992.
- Richter, A., Burrows, J. P., Nüß, H., Granier, C., and Niemeier, U.: Increase in tropospheric nitrogen dioxide over China observed from space, *Nature*, 437, 129–132, doi:10.1038/nature04092, 2005.
- Streets, D. G., Bond, T. C., Carmichael, G. R., Fernandes, S. D., Fu, Q., He, D., Klimont, Z., Nelson, S. M., Tsai, N. Y., Wang, M. Q., Woo, J.-H., and Yarber, K. F.: An inventory of gaseous and

- primary aerosol emissions in Asia in the year 2000, *J. Geophys. Res.*, 108(D21), 8809, doi:10.1029/2002JD003093, 2003.
- Sudo, K., Takahashi, M., Kurokawa, J., and Akimoto, H.: CHASER: a global chemical model of the troposphere – 1. Model description, *J. Geophys. Res.-Atmos.*, 107(D17), 4339, doi:10.1029/2001JD001113, 2002.
- Tanimoto, H., Sawa, Y., Matsueda, H., Uno, I., Ohara, T., Yamaji, K., Kurokawa, J., and Yonemura, S.: Significant latitudinal gradient in the surface ozone spring maximum over East Asia, *Geophys. Res. Lett.*, 32, L21805, doi:10.1029/2005GL023514, 2005.
- Uno, I., Ohara, T., Sugata, S., Kurokawa, J., Furuhashi, N., Yamaji, K., Tanimoto, N., Yumimoto, K., and Uematsu, M.: Development of RAMS/CMAQ Asian scale chemical transport modeling system, *J. Japan Soc. Atmos. Environ.*, 40(4), 148–164, [in Japanese], 2005.
- van Noij, T. P. C., Eskes, H. J., Dentener, F. J., et al.: Multi-model ensemble simulations of tropospheric NO<sub>2</sub> compared with GOME retrievals for the year 2000, *Atmos. Chem. Phys.*, 6, 2943–2979, 2006.
- van der A, R. J., Peters, D. H. M. U., Eskes, H., Boersma, K. F., Van Roozendaal, M., De Smedt, I., and Kelder, H. M.: Detection of the trend and seasonal variation in tropospheric NO<sub>2</sub> over China, *J. Geophys. Res.*, 111, D12317, doi:10.1029/2005JD006594, 2006.
- Yamaji, K., Ohara, T., Uno, I., Tanimoto, H., Kurokawa, J., and Akimoto, H.: Analysis of seasonal variation of ozone in the boundary layer in East Asia using the Community Multi-scale Air Quality model: What controls surface ozone level over Japan?, *Atmos. Environ.*, 40, 1856–1868, 2006a.
- Yamaji, K.: Modeling study of spatial-temporal variations of tropospheric ozone over East Asia, Ph. D. thesis for Kyushu University, 2006b.
- Zhang, M.-G., Uno, I., Sugata, S., Wang, Z.-F., D. W., and Akimoto, H.: Numerical study of boundary layer ozone transport and photochemical production in east Asia in the wintertime, *Geophys. Res. Lett.*, 29, 1545, doi:10.1029/2001GL014368, 2002.